

OPTICS ELEMENTS FOR MODELING ELECTROSTATIC LENSES AND ACCELERATOR COMPONENTS I. EINZEL LENSES

George H. Gillespie^a and Thomas A. Brown^b

^aG. H. Gillespie Associates, Inc., P.O. Box 2961, Del Mar, CA 92014, U.S.A.

^bCenter for Accelerator Mass Spectrometry, LLNL, P.O. Box 808, Livermore, CA 94551, U.S.A.

Abstract

A set of optical models for a variety of electrostatic lenses and accelerator columns has been developed for the computer code TRACE 3-D. TRACE 3-D is an envelope (matrix) code including space charge often used to model bunched beams in magnetic transport systems and radiofrequency (RF) accelerators when the effects of beam current may be important. Several new matrix models have been developed that allow the code to be used for modeling beam lines and accelerators with electrostatic components. The new models include (1) three einzel lenses, (2) two accelerator columns, (3) three electrostatic deflectors (prisms), and (4) an electrostatic quadrupole. A prescription for setting up the initial beam appropriate to modeling 2-D (continuous) beams has also been developed. The new models for (1) are described in this paper, selected comparisons with other calculations are presented, and a beamline application is summarized.

1. INTRODUCTION

TRACE 3-D uses the first-order transfer matrix (R-matrix) formalism to compute changes to the beam matrix (σ -matrix) [1]. However, rather than using the R-matrix for an entire optical element, TRACE 3-D divides each element into a series of small (longitudinal) segments and the calculation then steps through the beamline one segment at time. The effective transfer matrix may be modified in each segment.

The capability of TRACE 3-D to model longitudinal changes in parameters within an element allows one to include effects that are not possible with a strictly first-order code; e. g., space charge forces (applying impulses at each step) and permanent magnet quadrupole fringe field effects are included in the standard version of TRACE 3-D [1]. This "longitudinal" capability has been used in this work to incorporate changes in the beam energy as a function of position in the electrostatic elements, as well as to calculate fringe fields and retain the space charge model for all elements.

Three different electrode geometries for einzel (or unipotential [2]) lenses have been modeled and are illustrated in Figure 1. All of the lenses have cylindrical symmetry about the z axis, indicated by the dashed line in Figure 1. In addition, the einzel lenses are symmetric about their mid-points, corresponding to the point $z = 0$.

2. OPTICS MODELING

The optics of particles near the axis of cylindrically symmetric electrostatic elements is determined by the axial potential distribution $V(z)$. The first-order electric fields are given by

$$E_x(x,y,z) = + [(1/2) (\partial^2 V(z)/\partial^2 z)]x \quad , \quad (1)$$

$$E_y(x,y,z) = + [(1/2) (\partial^2 V(z)/\partial^2 z)]y \quad , \quad (2)$$

and

$$E_z(x,y,z) = - (\partial V(z)/\partial z) \quad . \quad (3)$$

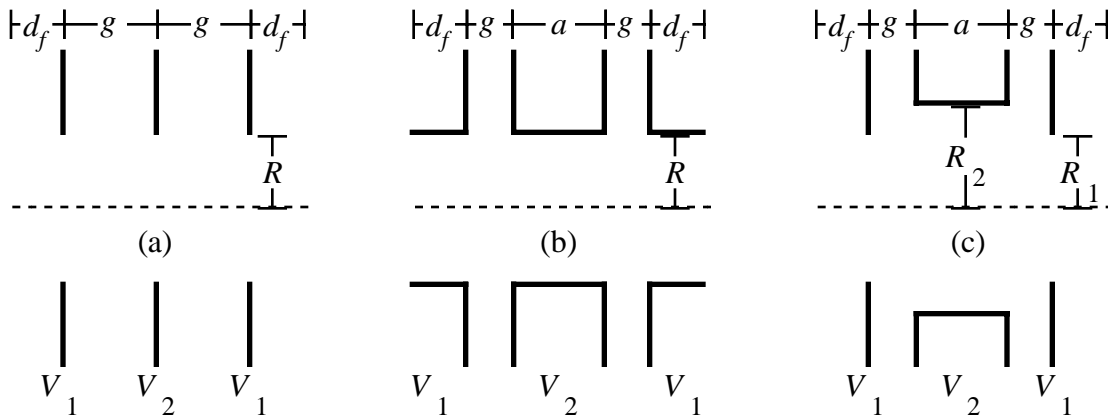


Figure 1. Electrode geometries for the three einzel lens models. Different potential functions are used to describe (a) a three-aperture lens, (b) a three-tube lens and (c) a two-aperture, center-tube lens.

The fields given above satisfy Maxwell's equation $\nabla \cdot \mathbf{E} = 0$ for any $V(z)$. The R-matrices describing the first-order optics may be computed directly from these fields. Our method follows that given in reference [3].

2.1 R-Matrix Elements

The region over which the fields (1)-(3) act is divided into small steps of length Δz and two R-matrices are computed for each step. The first R-matrix, together with an increase in the beam energy, computes the effects of a uniform electric field acting over a distance of Δz . The non-trivial elements of this R-matrix are

$$R_{13} = R_{24} = 2\Delta z / [1+(\eta_-)^{1/2}] \quad , \quad (4)$$

$$R_{22} = R_{44} = R_{66} = 1/(\eta_-)^{1/2} \quad , \quad (5)$$

and

$$R_{56} = \Delta z / \gamma^2 \quad , \quad (6)$$

where

$$\eta_- = V(z)/V(z - \Delta z) \quad , \quad (7)$$

and γ is the relativistic energy factor of the beam at z .

The second R-matrix computes the effective thin lens for the focusing effect of the field applied as an impulse. The non-trivial elements of this R-matrix are

$$R_{21} = R_{43} = -[\eta_+ \eta_- - 2\eta_- + 1]/(4\eta_- \Delta z) \quad , \quad (8)$$

where

$$\eta_+ = V(z + \Delta z)/V(z) \quad . \quad (9)$$

The formulas given by Equations (4)-(9) can be used to model any electrostatic element whose potential is given at discrete positions on the axis. In this work, analytic forms for the on-axis potential functions are used for computing the R-matrix elements.

2.2 Potential Functions

The potential as a function of z for the einzel lenses illustrated in Figure 1 may be written in terms of the electrode potentials V_1 and V_2 as

$$V(z) = V_1 + [(V_2 - V_1)/2] \phi(z) \quad , \quad (10)$$

where $\phi(z)$ is an even function of z , and goes to zero as z approaches $\pm\infty$. The function $\phi(z)$ depends only on the geometry (electrode spacings and dimensions) of the lens.

For the three-aperture lens illustrated in Figure 1(a), we use a potential that is a special case of the potential for the two-aperture center-tube lens, Figure 1(c). (That potential is described further below.) When the two radii are equal, and the center tube has the zero length, the formula for $\phi(z)$ is given by

$$\phi(z) = (2/\pi)(g)^{-1} \{A\} \quad , \quad (11)$$

where

$$A = (z+g)\tan^{-1}[(z+g)/R] + (z-g)\tan^{-1}[(z-g)/R] - (2z)\tan^{-1}[(z)/R].$$

For the three-tube lens illustrated in Figure 1(b), we use the following formula for $\phi(z)$

$$\phi(z) = R(\omega'g)^{-1} \ln\{A/B\} \quad , \quad (12)$$

where

$$A = [\cosh(2\omega z/R) + \cosh[(\omega a/R) + (\omega'g/R)]] \quad , \quad (13)$$

and

$$B = [\cosh(2\omega z/R) + \cosh[(\omega a/R) - (\omega'g/R)]] \quad . \quad (14)$$

The constants $\omega=1.31835$ and $\omega'=1.67$. This form of the potential is based upon a parameterization of a single two-cylinder (acceleration) lens [4]. The potential was obtained from the superimposition of potentials for 2 back-to-back, two-cylinder lenses, with the end electrodes set to V_1 , and the adjacent electrodes set to V_2 [5]. When $\omega'=\omega=1.318$, the potential given by (12)-(14) is the same as that used by Lu, Ben-Zvi and Cramer [3] and other authors. The use of $\omega'=1.67$ provides better agreement with numerical solutions to Laplace's equation for certain cases [4].

For the two-aperture center-tube lens illustrated in Figure 1(c), we use a potential given by El-Kareh and El-Kareh; see Equation (6.5) of reference [2]. Specifically,

$$\phi(z) = (2/\pi)(g)^{-1} \{A-B\} \quad , \quad (15)$$

where

$$A = (z+g+a/2)\tan^{-1}[(z+g+a/2)/R_1] + (z-g-a/2)\tan^{-1}[(z-g-a/2)/R_2] + 2R_1 \quad , \quad (16)$$

and

$$B = (z+a/2)\tan^{-1}[(z+a/2)/R_1] + (z-a/2)\tan^{-1}[(z-a/2)/R_2] + 2R_2 \quad . \quad (17)$$

When $R_1 = R_2 = R$ and $a = 0$, these results reduce to that given by Equation (11) above.

The fields are modeled to a distance d_f before and after each lens, so that the full length of a lens is $2(g+d_f)+a$. In the calculations described here, the value of $d_f = fR$ (or fR_1), where f is the TRACE 3-D fringe field extension factor, PQEXT [1].

3. COMPARISONS WITH OTHER WORK

Several calculations have been carried out using the einzel models described above for comparison to other results available in the literature. Table 1 gives the focal length f obtained from TRACE 3-D for the 3-tube lens, together with results from numerical calculations by Adams and Read [5], all expressed as the ratio $f/(2R)$.

Table 1. Focal length to aperture ratio for 3-tube einzel lenses. Results for two fringe field factors f are given.

V_2/V_1	$f/(2R) = -1/[2R R_{21}]$ [this work]		$f/(2R)$ [5]
	$f=2.5$	$f=10.0$	
-0.5	0.632	0.629	0.628
0.0	2.832	2.842	2.843
0.8	131.524	141.267	141.752
2.0	11.462	11.169	11.261
9.0	1.288	1.301	1.312

4. BEAMLINe DIAGNOSTIC APPLICATION

The three-tube einzel lens model described above has been used in developing a diagnostic model of the low-energy injection system for the Center for Accelerator Mass Spectrometry (CAMS) at the Lawrence Livermore National Laboratory (LLNL). Figure 2 illustrates a TRACE 3-D simulation of the injection beamline. In the first step of the model development, iterative adjustment of the TRACE 3-D source emittance and voltage on the second einzel lens of the zoom-lens section (element 6 in Figure 2) resulted in a simulation of the beamline that was consistent with measured beam profiles at the equivalent of positions 4/5 and 7/8 in Figure 2 (the first einzel lens was turned off for this test).

The second einzel lens voltage required in the model to produce a beam waist at position 7/8 was 27.4 kV. This value is within 1.5% of the measured 27.8 kV required in the laboratory. Given the uncertainties in the DAC/ADC conversion factors, the difference between the two values is not significant. Since the superposition derivation of Equation (12) is valid for $g/a \leq 1/3$ and $a/2R \geq 1/2$, and the physical dimensions of the second einzel lens are such that $a/2R = 1.1$ and $g/a = 0.1$, this level of agreement was expected.

In the second step of this development, a full model of the injection system has been constructed. This model has been used in understanding and optimizing the transport of various ions through the low-energy injection system and into the CAMS accelerator.

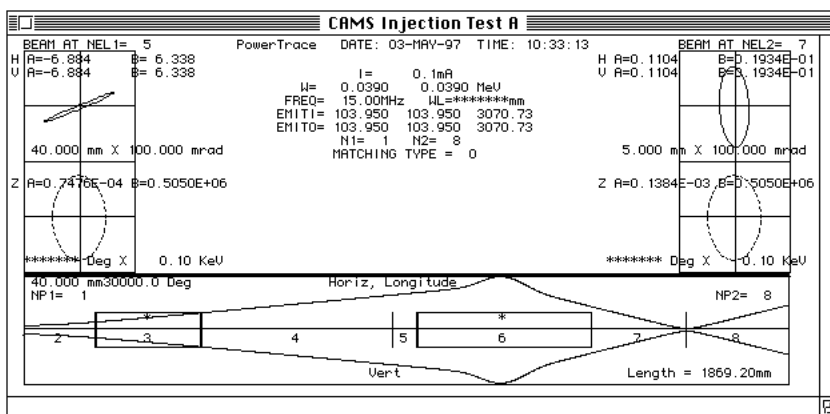


Figure 2. TRACE 3-D output for the zoom-lens section of the modeled low-energy injection line. This figure shows the results obtained after adjustment of the source emittance and second einzel lens voltage to match the measured beam profiles at the equivalent of positions 4/5 and 7/8.

5. SUMMARY

Several optical elements for electrostatic accelerator devices have been developed. The elements have been integrated into a version of the TRACE 3-D code that works within the Shell for Particle Accelerator Related Codes (S.P.A.R.C.) software environment [6]. A detailed summary of the einzel models used for the code has been presented. Focal length calculations show good agreement with other results from the literature. The utility and accuracy of the einzel lens models has been demonstrated in the development of a diagnostic model of the low-energy injection line at the LLNL Center for Accelerator Mass Spectrometry. Details for other elements will be published in future papers.

ACKNOWLEDGMENTS

The assistance of Barry W. Hill in developing new components for the S.P.A.R.C. interface is gratefully acknowledged. This work performed in part under the auspices of the U.S. Department of Energy at the Lawrence Livermore National Laboratory under contract W-7405-Eng-48.

REFERENCES

- [1] K. Crandall and D. Rusthoi, "TRACE 3-D Documentation," Los Alamos National Laboratory Report LA-UR-90-4146, 92 pages (1990).
- [2] A. B. El-Kareh and J. C. J. El-Kareh, Chapter VI "The Electrostatic Unipotential Lens," *Electron Beams, Lenses and Optics*, Vol. 1, Academic Press, New York, 186--228 (1970).
- [3] J.-Q. Lu, I. Ben-Zvi and J. G. Cramer, "LYRAN A Program for the Analysis of Linac Beam Dynamics" *Nucl. Instru. Meth. Phys. Res. A* **262**, 200-6 (1987).
- [4] F. H. Read, A. Adams and J. R. Soto-Montiel, "Electrostatic Cylinder Lenses I Two Element Lenses," *J. Phys. E* **4**, 625-632 (1971).
- [5] A. Adams and F. H. Read, "Electrostatic Cylinder Lenses II Three Element Einzel Lenses," *J. Phys. E* **5**, 150-155 (1972).
- [6] G. H. Gillespie and B. W. Hill, "A Graphical User Interface for TRACE 3-D Incorporating Some Expert System Type Features," 1992 Linear Accelerator Conference Proc., AECL-10728, 787-789 (1992).